Electronic Supplementary Information (ESI)

Superior High-rate Performance of Core-shell $Li_4Ti_5O_{12}$/Carbon Nanocomposite Synthesized by a Supercritical Alcohol Approach

*Agung Nugroho, Wonyoung Chang, Su Jin Kim, Kyung Yoon Chung, and Jaehoon Kim**

Synthesis of $Li_4Ti_5O_{12}$

14.27 mg of $LiOH·H_2O$ (purity 98 wt%, Sigma-Aldrich, St Louis, MO, USA), 56.9 mg of oleylamine (purity 70 wt%, Sigma-Aldrich), and 122.1 mg of TTIP (purity 97 wt%, Sigma-Aldrich) were charged into 3.5 mL of MeOH and the suspension was transferred into an SUS316 tube reactor with an inner volume of 11 mL. The reactor was then heated in a molten-salt bath at 400 °C. After 15 min, the resulting precipitates were washed carefully with MeOH to remove residual organic species followed by vacuum drying at 100 °C for 12 h. The samples, referred to as LTO-OA1 and LTO-OA2, were calcined at a temperature of 750 °C for 5 h in an Ar/5% H_2 flow. The calcined samples are referred to as LTO-OA1-750C and LTO-OA2-750C, respectively. The micron-sized LTO sample prepared using a solid-state method is referred to as LTO-SS. The submicron-sized LTO sample prepared in supercritical water with subsequent calcination in air at 700 °C is referred to as LTO-scH_2O-700C. Detailed synthetic conditions were described in our previous paper.[1] The LTO sample prepared in scMeOH with subsequent calcination in air at 600 °C is referred to as LTO-scMeOH-600C.

Characterization

The crystal structures of the samples were characterized using XRD (Rigaku RINT2000, Tokyo, Japan) with Cu Kα radiation at 40 kV and 50 mA. The organic functional groups on the surface of LTO were characterized using a NICOLET 380 FT-IR spectrometer (Thermo Electron Co. NJ, USA). The thermal properties of the obtained particles were measured using a DuPont Instruments TGA 2950 thermal gravimetric analyzer. The particle morphologies were observed using HR-TEM (Tecnai FT20, FEI Co., OR, USA). The electrochemical performance of the sample was tested using a Type CR2032 coin cell (counter electrode: Li metal, electrolyte: 1 M $LiPF_6$ dissolved in ethylene carbonate (EC)/dimethyl carbonate (DMC)/ethyl methyl carbonate (EMC), volume ratio of EC/DMC/EMC = 1:1:1, weight ratio of LTO/carbon black/poly(vinylidene fluoride) = 87:8:5). The cells were galvanostatically charged and discharged in the voltage range from 1.0 to 2.5 V (*vs.* Li/Li^+) using a MACCOR Series 4000 Battery Test System (OK, USA).

Table S1. Different synthesis and coating methods of carbon-coated LTO and its electrochemical performance

Samples	LTO Synthesis method	Carbon coating method	Calcination condition	LTO size/LTO morphology/coating content/coating thickness/coating structure	Cell composition (active material:AB:binder) and Working voltage	Discharge capacity (mAh/g)	Refs
LTO/C[a]	Supercritical methanol	Carbonization from oleyamine modified LTO	750 °C, 6 h, in Ar+H$_2$	5-15 nm/ nanoparticle/ 6-14%/ 0.7-2.3 nm/ layer	87:8:5 1.0-2.5 V	147 (at 10C) 139 (at 20C) 128 (at 30C) 101 (at 50C)	This study
LTO/Ti(III)/C[b]	Solid-state	*In situ* polymerization of aniline	800 °C, 24 h, in Ar+H$_2$	50-70 nm/ nanoparticle/3%/NA /NA	80:15:5 1.0-3.0 V	115 (at ~ 10C) 75 (at ~ 20C)	Wang et al., 2009[2]
LTO/C-N[c]	Spray-drying	Pyrolysis of urea	400 °C, 30 min, in Ar+H$_2$	NA/porous/NA/ 2 nm/thin layer	80:10:10 1.0-2.2 V	105 (at 10C)	Pan et al., 2012[3]
LTO/C-N[d]	Spray-drying	Pyrolysis of ionic liquid	600 °C, in Ar	NA/porous/7%/ 2-3 nm/thin layer	80:10:10 1.0-2.2 V	129 (at 10C)	Zhao et al., 2011[4]
LTO/C[e]	Solid-state	Thermal vapor decomposition of toluene	800 °C, 2 h, in N$_2$	NA/nanoparticle/3% /3-5 nm/thin layer	90:5:10 1.0-3.0 V	12.5 (at 20C)	Cheng et al., 2007[5]
LTO/C[f]	Solid-state	Chemical vapor deposition	800 °C, in inert	50-80 nm/nanorod/ 3% /5 nm/thin layer	90:5:10 1.0-3.0 V	140 (at 10C) 120 (at 20C)	Cheng et al., 2010[6]
LTO/C[g]	Anionic Polymerization	Self assembly block coplymer	700 °C, 2 h, in N$_2$	NA/mesostructure/ 8.5% /NA/thin layer	80:10:10 1.0-2.5 V	115 (at 10C) 90 (at 50C)	Kang et al., 2011[7]
LTO/C[h]	High-energy ball-miling assited solid-phase	Carbonization from sucrose	750 °C, 5 h, in Ar+H$_2$.	20-30 nm/ nanoparticle/4.3%/ 1-3 nm /thin layer	85:8:7 1.0-3.0 V	121 (at 10C) 110 (at 20C) 90 (at 40C)	Yuan et al., 2011[8]

LTO/C[i]	Spray drying	Pyrolysis of $C_{28}H_{16}Br_2$	400 ^{o}C	50 nm/ porous microsphere/ 5.9% / 1 nm /ultrathin layer	80:10:10 1.0-2.2 V 1.0-3.0 V	131 (at 5C) 104 (at 10C)	Jian et al., 2012[9]
LTO/C[j]	Spray drying	Carbonization of sugar	800 ^{o}C, 10 h, in N_2	200 nm/ porous microsphere/ 6% /6nm /thin layer	85:5:10 1.0-3.0 V	129 (at 10C) 126 (at 20C)	Zhu et al., 2011[10]
LTO/C[k]	Sol-gel	Pyrolysis of citric acid	800 ^{o}C, 15 h in Ar	200-700 nm/ nanoparticle/2-5%/ 2-10 nm /thin layer	85:10:5 1.0-3.0 V	~ 100 (at 5C)	Wang et al., 2011[11]
LTO/C[l]	Cellulose-assisted combustion process	Carbonization from sucrose	700 °C for 5 h in air	700-900 nm/ microparticle/ 3.35% /5 nm /thin layer	85:8:7 1.0-2.0 V	~ 130 (at 10C)	Yuan et al., 2010[12]
LTO/C[m]	Solid state method	Carbonization of multiwall CNT	800 °C for 10 h in Ar	NA/microparticle/ 3.04% /NA/NA	85:10:5 1.0-3.0 V	134 (at 10C)	Li et al., 2010[13]
LTO/C[n]	Rheological phase method	Polyvinylbutyral as template and carbon source	800 °C for 15 h in Ar	2.1 µm/ microparticle/0.98% / NA/thin layer	80:10:10 1.0-2.6 V	127 (at 3C)	Liu et al., 2008[14]
LTO/C[o]	Solid state method	Carbonization of sugar	850 °C for 24 h in air	NA/microparticle/ NA/NA/NA	80:10:10 1.0-2.5 V	40 (at 2C)	Wang et al., 2007[15]
LTO/C/CNT[p]	Solid state method	Carbonization using pitch and CNT	800 °C for 12 h in Ar	NA/microparticle /6%/NA/NA	92:3:5 1.0-3.0 V	143 (10C)	Li et al., 2010[16]
LTO/C[q]	Solid state method	Carbonization using PAA, CA, MA, PVA	800 °C for 8 h in N_2	0.1-1 µm/ microparticle/ 3-4.5% /NA/NA	86:10:4 1.0-3.0 V	133 (10C)	Hu et al., 2011[17]
LTO/P[r]	Thermal decomposition	Thermal decomposition of trioctylphosphine	600 ^{o}C, 2 h, in $Ar+H_2$.	30-52 nm/ nanoparticle/NA/NA /NA	80:11:9 1.0-3.0 V	100 (at 10C)	Jo et al., 2011[18]

LTO/N[s]	Thermal Nitridation	Thermal nitridation using NH_3	700 °C, 1 h, in NH_3.	NA/nanoparticle/NA/NA/NA	82:10:8 1.0-3.0 V	120 (at 10C)	Park et al., 2008[19]
LTO[t]	Solution-combustion method	NA		20-50 nm/ nanoparticle/NA/NA/NA	80:15:5 1.0-2.0 V	140 (at 10C) 102 (at 50C)	Prakash et al., 2010[20]
LTO[u]	Microwave-assisted hydrothermal	NA	550 °C, 6 h, in Air	500-800 nm/ nanoparticle/NA/NA/NA	80:10:10 1.0-3.0 V	100 (at 10C) 62 (at 40C)	Chou et al., 2011[21]
LTO[v]	Thermal method	NA	800 °C, 3 h	80-100 nm/nanowire/ NA/NA/NA	90:5:5 1.0-2.5 V	155 (at 10C)	Kim et al., 2007[22]

[a] Surface-modified LTO was synthesized in supercritical methanol with $Ti(OCH_3O_7)_4$ and LiOH as the LTO precursors and oleylamine as the surface-modifier. The surface-modified LTO was calcinated in in Ar+5% H_2 at 750 °C to obtained carbon-coated LTO.

[b] Polyaniline coated with TiO_2 was prepared by hydrolysis of $Ti(OCH_3O_7)_4$ coupled with polymerization of aniline. The mixture was solid-state reacted and calcinated at 800 °C for 24 h in Ar+5% H_2.

[c] Porous LTO was synthesized using spray-drying method. The LTO powders were mixed with urea aqueous solution. After drying, the mixture was heated to 400 °C for 30 min in Ar.

[d] Porous LTO was synthesized using spray-drying method. The LTO powders were mixed with an ionic liquid (1-ethyl-3-methylimidazolium dicyanamide). The mixture was calcinated at 600°C in Ar.

[e] LTO was synthesized by the solid-state method from TiO_2 and Li_2CO_3 as the precursors. The LTO particles were carbon-coated via thermal decomposition of toluene at 800°C for 2 h in N_2.

[f] Carbon-coated LTO was synthesized by chemical vapor deposition (CVD) followed by the solid-state method. The TiO_2 is first coated with conductive carbon layer by CVD method. Then the carbon coated precursor was mixed with lithium salt followed by heat treatment in inert atmosphere at 800°C.

[g] Mesostructured spinel LTO-carbon nanocomposite with uniform pore size were synthesized via anionic polymerization using poly(isoprene)-b-poly(ethylene oxide) block-copolymer (PI-b-PEO). The LTO particles were carbon-coated via thermal treatment at 700°C for 2 h in N_2.

[h] LTO was synthesized by high energy ball milling assisted solid state reaction using TiO_2 and Li_2CO_3 as the precursors. The LTO particles were carbon-coated via thermal decomposition of sucrose at 800 °C for 5 h in N_2.

[i] Porous LTO microsphere first prepared by spray drying method with $C_{28}H_{16}Br_2$. Porous LTO coated with carbon was then prepared via the low-temperature pyrolysis of $C_{28}H_{16}Br_2$ at 400 °C.

[j] Carbon-coated and nanosized LTO nanoporous microsphere was synthesized by carbon pre-coating process using anatase TiO_2 and sugar combined with spray drying to form carbon-coated TiO_2. The obtained powder was mixed with Li_2CO_3 using ball milling. The resulted product was annealed at 800 °C for 10 h in N_2.

[k] Carbon-coated LTO was synthesized by sol-gel method using citric acid as a carbon source. LTO particles were carbon-coated via thermal treatment at 800°C

for 15 h in Ar.

[l] LTO/C was synthesized by the cellulose-assisted combustion technique from $Ti(OCH_2CH_2CH_2CH_3)_4$ and $LiNO_3$ as the precursors with sucrose as a carbon source. The LTO particles were obtained via thermal treatment at 700 °C for 5 h.

[m] LTO/graphitized carbon nanotubes (GCNTs) composite was synthesized by the solid-state method from TiO_2 and CH_3COOLi as the precursors. The LTO/ GCNTs particles were obtained via thermal decomposition of multiwall carbon nanotubes at 800°C for 10 h in Ar.

[n] LTO/C was synthesized by the rheological phase method using polyvinylbutyral (PVB) as both a template and a carbon source. The LTO particles were obtained by thermal treatment of precursor (TiO_2 and Li_2CO_3) and PVB at 800 °C for 15 h in Ar.

[o] Carbon-coated spinel LTO was synthesized by the solid-state method from TiO_2 and Li_2CO_3 as the precursors and sugar as a carbon source. A nanolayer of amorphous carbon was coated on the surface of LTO after heat treatment at 850 °C for 24 h in air.

[p] LTO/C/CNTs composite was synthesized by the solid-state method from TiO_2 and Li_2CO_3 as the precursors, pitch as a carbon source, and carbon nanotubes (CNTs). The LTO particles were carbon-coated on CNT via thermal treatment at 800 °C for 12 h in Ar.

[q] LTO/C composites were synthesized by one-step, solid-state method from TiO_2 and LiOH as the precursors using organic compounds (citric acid (CA) and maleic acid (MA)) and polymers (polyacrylate acid (PAA) and polyvinyl alcohol (PVA)) as carbon sources. The LTO/C particles were obtained via thermal treatment at 800 °C for 8 h in N_2.

[r] LTO/P was produce by thermal treatment of commercial LTO and trioctylphospine (TOP). The phosphidation was produced during thermal treatment of TOP at 600 °C for 2 h in Ar.

[s] LTO/N was synthesized by the thermal nitridation from commercial nano-LTO as a precursor and NH_3 as a reducing agent. A surface conductive layer TiN on LTO particles were obtained by thermal nitridation of NH_3 at 700 °C for 1 h.

[t] Nanocrystalline LTO was synthesized by a solution combustion method from $TiO(NO_3)_2$ and $LiNO_3$ as precursors and glycine as a fuel. All the precursors were taken in alumina crucible and placed into a furnace preheated to 800 °C.

[u] LTO was synthesized by a microwave-assisted hydrothermal method from $Ti(OCH_3O_7)_4$ and LiOH as precursors. Microspheres LTO particles were obtained after post annealing at 550 °C for 5 h in air.

[v] LTO nanowires was synthesized by the firing a mixture of TiO_2 nanowires and Li acetate at 800 °C for 3 h.

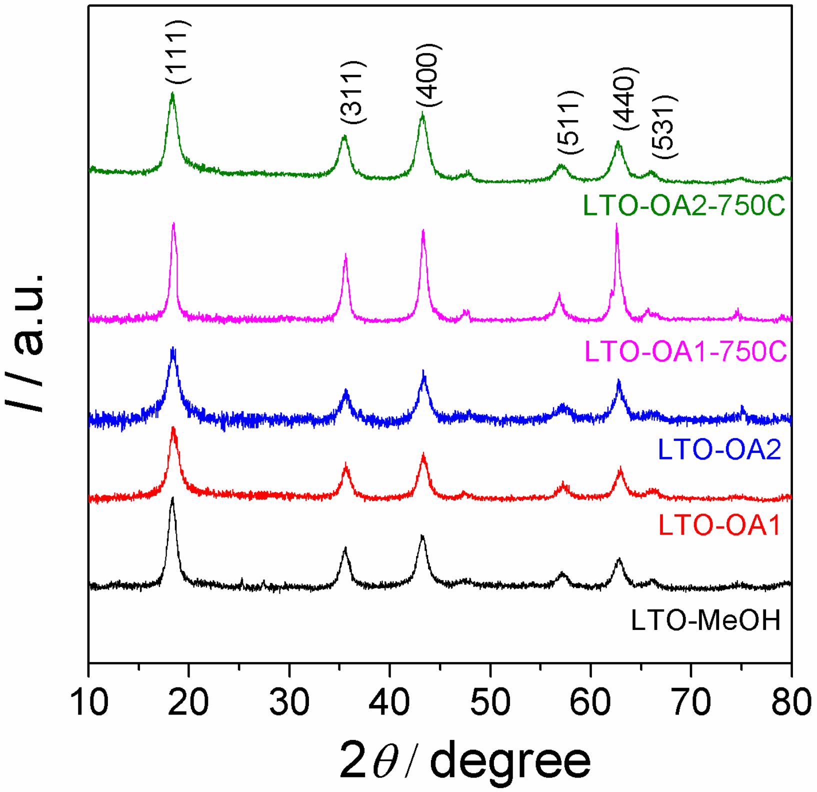

Fig. S1. The powder X-ray diffraction patterns of LTO-scMeOH, LTO-OA1, LTO-OA2, LTO-OA1-750C and LTO-OA2-750C.

The powder X-ray diffraction (PXRD) patterns of unmodified LTO (LTO-scMeOH), oleylamine-modified LTO (LTO-OA1 and LTO-OA2) synthesized in supercritical methanol (scMeOH), and core-shell LTO/C nanocomposite (LTO-OA1-750C and LTO-OA2-750C) by the calcination of the oleylamine-modified LTO at 750 °C in an Ar+5% H_2 flow. Titanium tetraisopropoxide (TTIP) was used as the Ti source. The mole ratio of TTIP:oleylamine was 10:1 for synthesizing the LTO-OA1 sample and was 10:8 for synthesizing the LTO-OA2 sample. All main diffraction peaks observed for the synthesized particles can be assigned to spinel LTO pattern (JCPDS No.49-0207), indicating highly phase-pure LTO was synthesized in scMeOH at the short reaction time of 15 min. The crystallite size estimated using the Scherrer equation and (111) peak was estimated to be 4.9 nm, 4.2 nm, and 2.0 nm for LTO-scMeOH, LTO-OA1, and LTO-OA2 samples, respectively. After carbon layer formation onto LTO surface by the calcination, slight increase in the LTO crystallite size was observed; the crystallite size for LTO-OA1-750C and LTO-OA2-750C estimated to be 9.2 nm and 5.0 nm, respectively.

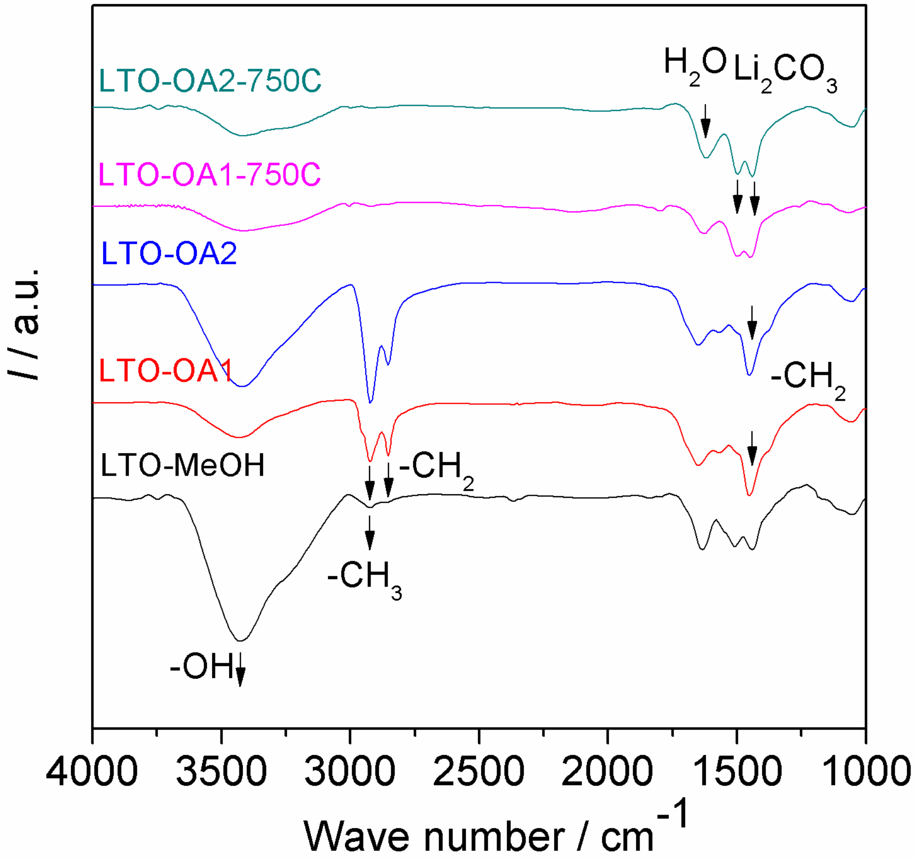

Fig. S2. Fourier transform infrared (FT-IR) spectroscopy of LTO-scMeOH, LTO-OA1, LTO-OA2, LTO-OA1-750C and LTO-OA2-750C.

The surface functional groups were examined by Fourier transform infrared (FT-IR) spectroscopy. The FT-IR spectra of the LTO-scMeOH exhibits methyl ($-CH_3$) stretching peak at 2926 cm^{-1} and -OH stretching peak at 3000-3750 cm^{-1}, suggesting that supercritical methanol acts as a methylation, hydroxylation, and methoxylation agent.[23-24] The presence medium stretching peak (2850 cm^{-1}) and strong bending peak (1450 cm^{-1}) of $-CH_2-$, and $-CH_3$ stretching peak at 2920 cm^{-1} in LTO-OA1 and LTO-OA2 indicates the presence of olelyamine on the LTO surface. After the calcination, the $-CH_2-$ and $-CH_3$ peaks disappeared. The peak of 1436 and 1498 cm^{-1} is associated with Li_2CO_3 which is attach on the surface due to reaction of remain LiOH with CO_2, while peak of 1621 cm^{-1} is bending mode of water molecule.[25-26]

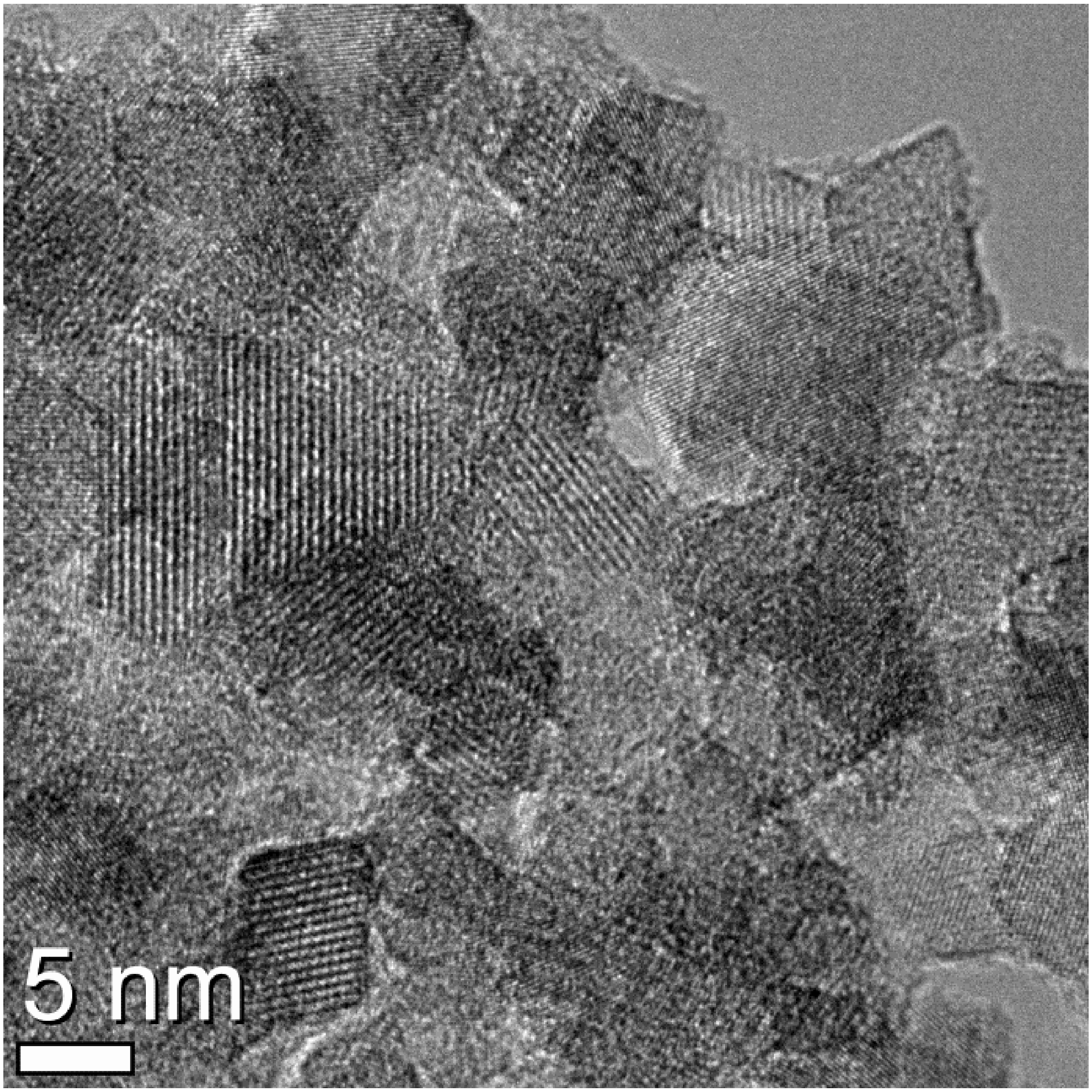

Fig. S3.HR-TEM image of LTO-OA1

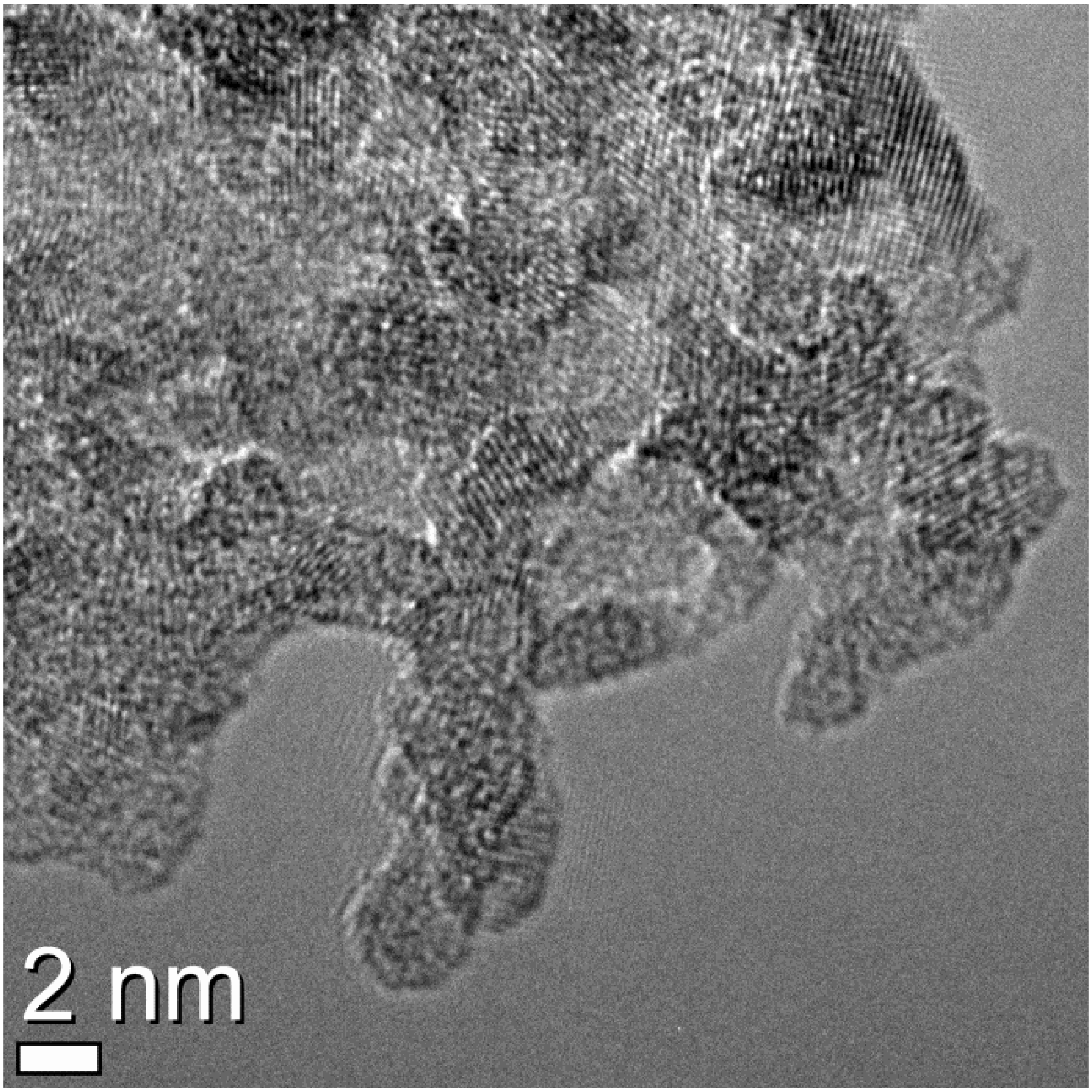

Fig. S4.HR-TEM image of LTO-OA2

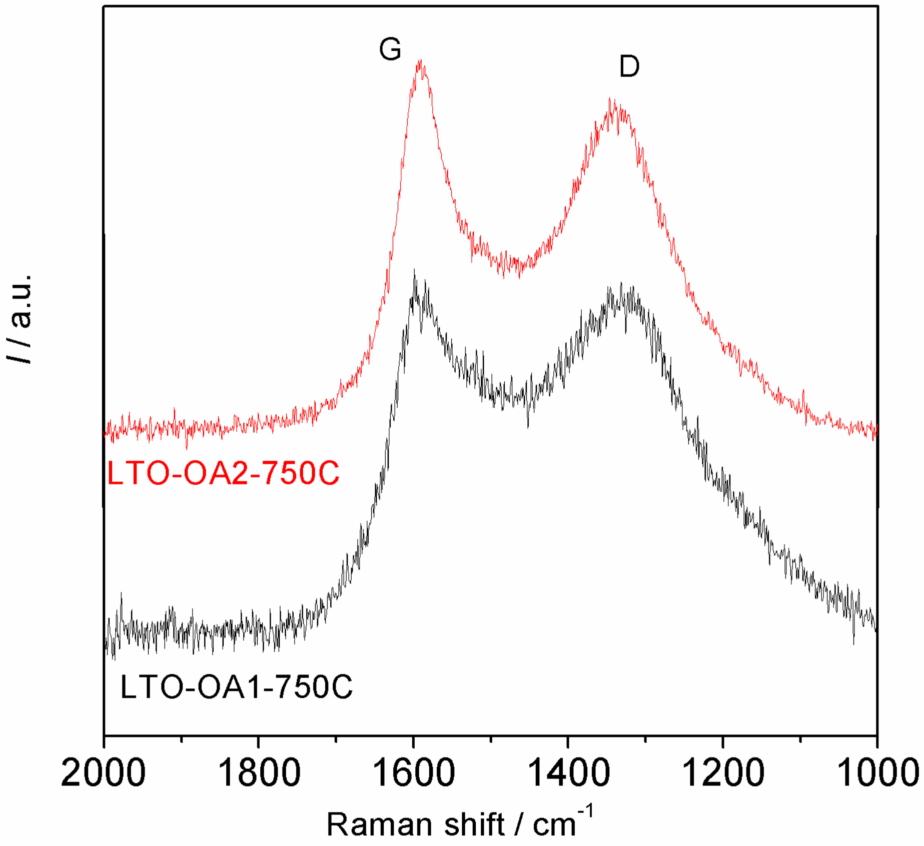

Fig. S5. Raman spectra of LTO-OA1-750C and LTO-OA2-750C.

The structure of the carbon in the LTO/C nanocomposites was monitored using Raman spectroscopy. The band at 1591 cm^{-1} is one of the E_{2g} modes (or G band, sp^2), which is associated with a graphene sheet. The band at 1338 cm^{-1} is one of the D bands (sp^3), which is an amorphous carbon band. The high I_D/I_G ratio indicates that the high content of graphitic carbon in the LTO/C sample.

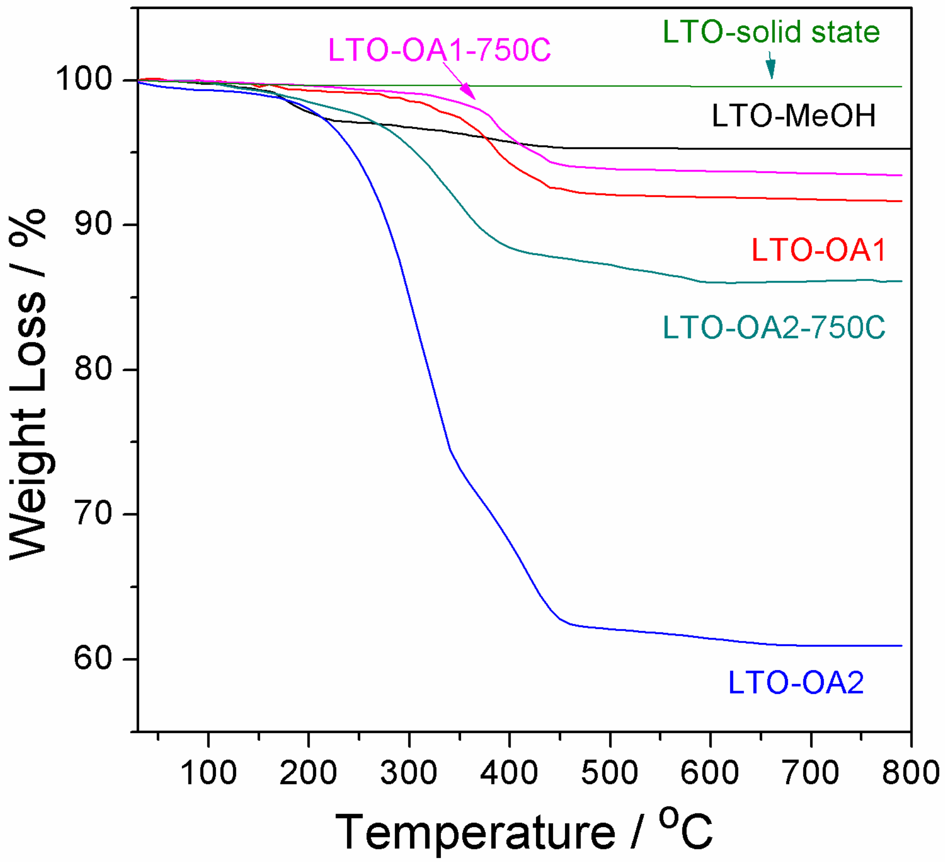

Fig. S6. Thermal gravimetric analysis of LTO-scMeOH, LTO-OA1, LTO-OA2, LTO-OA1-750C, LTO-OA2-750C, and LTO prepared by the solid-state method (LTO-solid state)

The weight loss of the samples is attributed to organic species burn-off in air flow. LTO-scMeOH retained weight loss of 4.7 % while much higher values of weight losses were observed in the LTO-OA1 (8.3 %) and LTO-OA2 (39.1 %) sample, indicating the surface of LTO-OA1 and LTO-OA2 samples were covered by the organic modifier. The degree of weight loss can correspond to the surface coverage of the surface modifiers. Considering the size, shape, and density of the produced LTO, the surface coverages of the LTO-OA1 and LTO-OA2 samples were estimated to be 11.1 % and 41.2 %, respectively.[24, 27-28] After the carbonization, the weight loss of LTO-OA1-750C and LTO-OA2-750C decreased to be 6.4 % and 14.0 %, respectively. These values can correspond to the carbon content in the LTO/C nanocomposites[5] since weight of bare LTO sample in the absence of organic species on the surface was negligible during calcination in air (LTO-solid state).

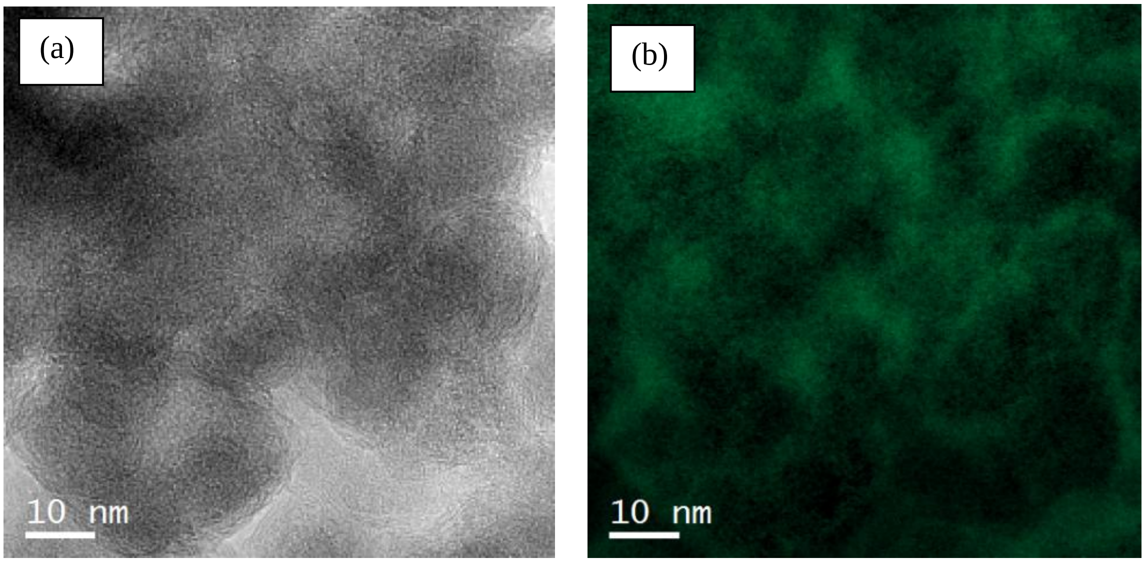

Fig. S7. (a) Zero-loss TEM image of core-shell LTO/C nanocomposite (LTO-OA2-750C). (b) The element map of carbon corresponding to LTO/C nanocomposite (LTO-OA2-750C). Green area is carbon-rich phase. Zero-loss image was recorded using a 10 eV slit. The distribution of carbon in the LTO/C nanocomposite was investigated by an energy-filtered transmission electron microscopy (EF-TEM) imaging. (Carbon K edge at 284 eV, slit width: 20 eV)

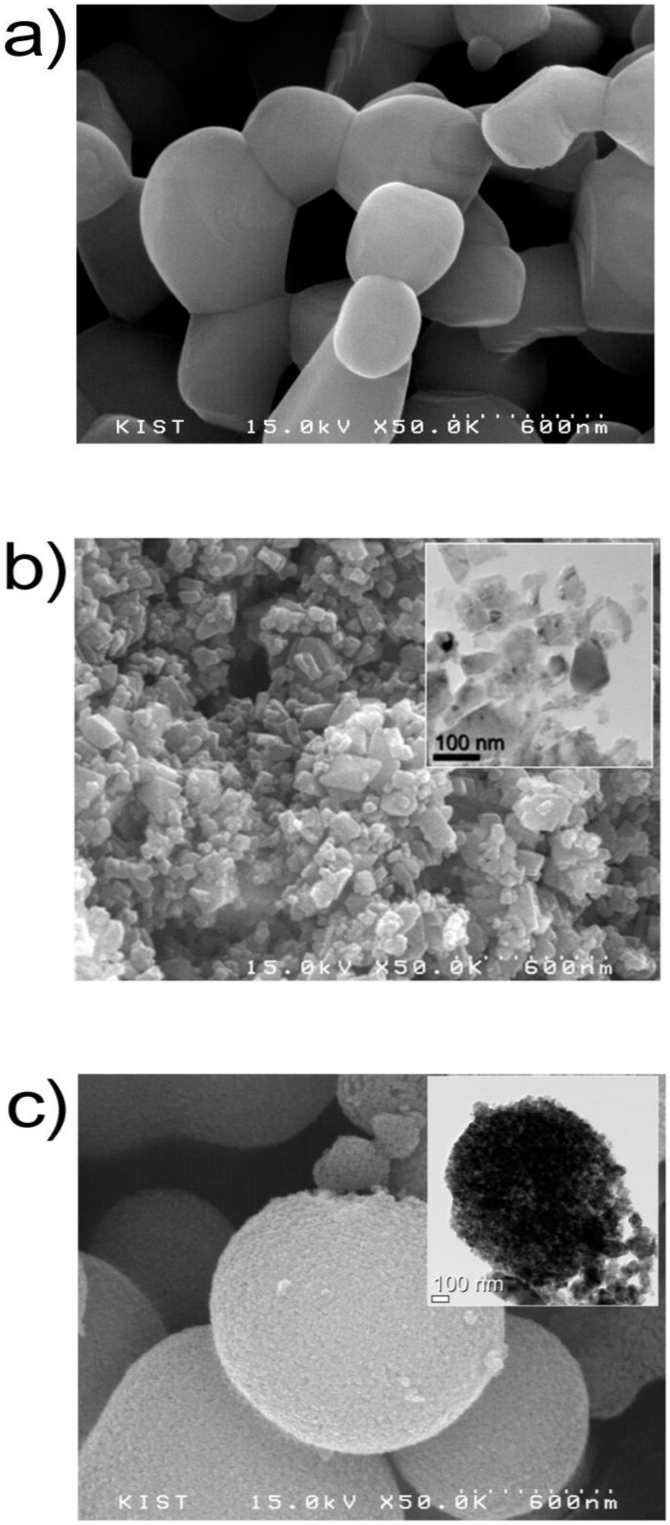

Fig. S8. SEM or TEM image of (a) LTO-SS, (b) LTO-scH_2O-700C, and (c) LTO-scMeOH-600C

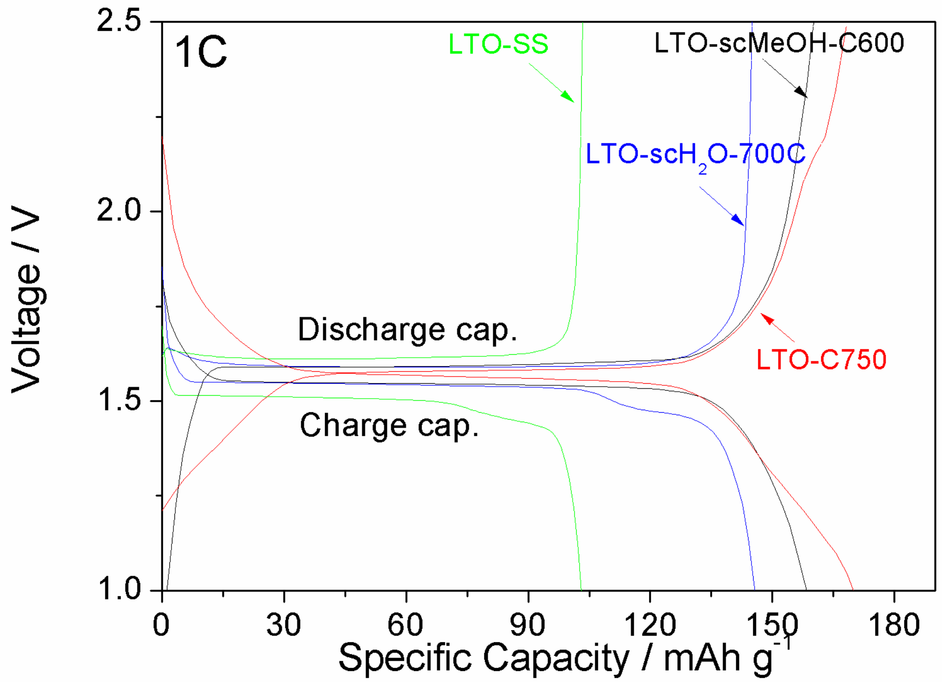

Fig. S9. The galvanostatic discharge/charge curves for Li insertion-extraction of each sample at 1 C

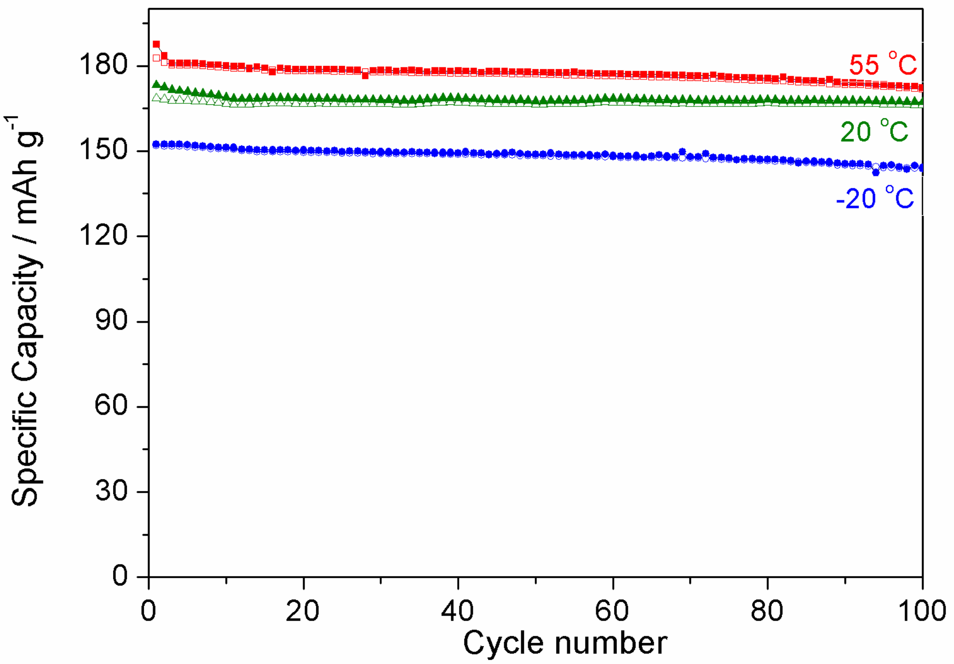

Fig. S10. The cyclability of the core-shell LTO/C nanocomposite (LTO-OA2-750C) at different testing temperatures.

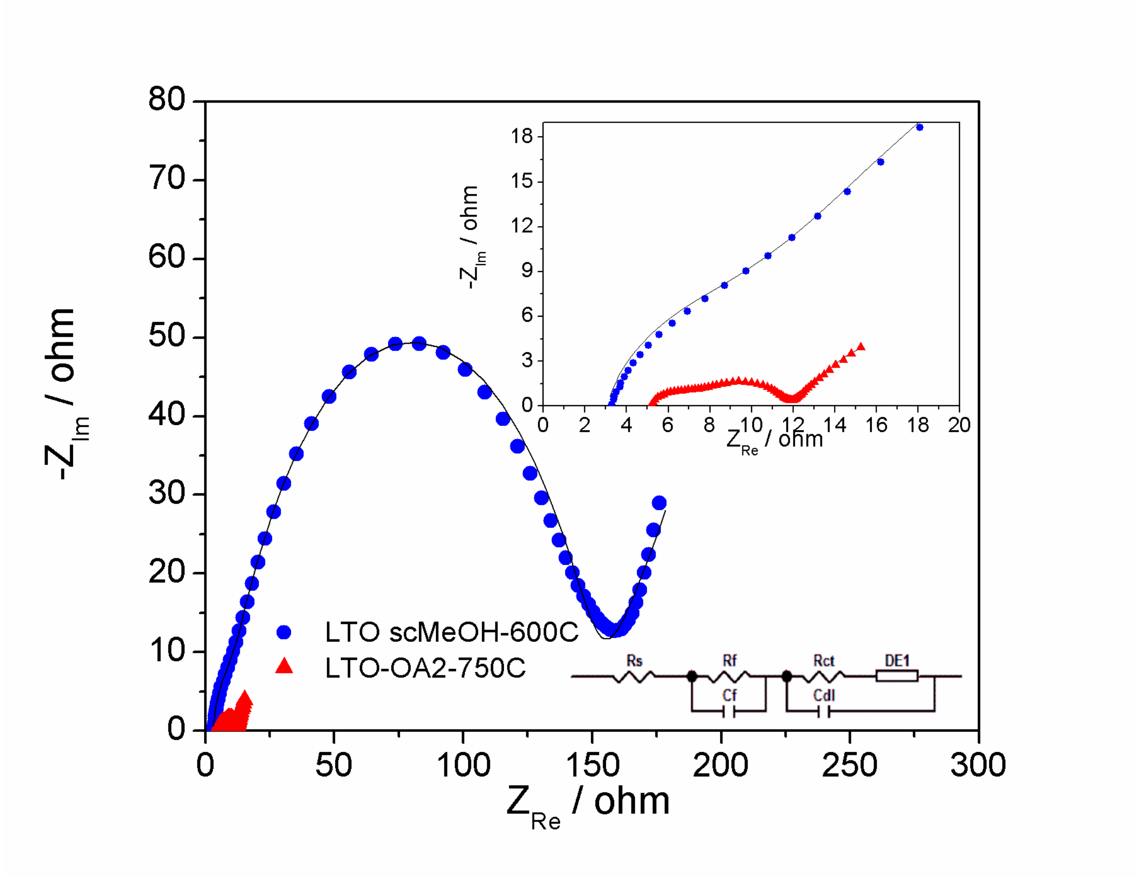

Fig. S11. Impedance spectra of the uncoated, mesoporous LTO (LTO-scMeOH-600C) and core-shell LTO/C nanocomposite (LTO-OA2-750C). The LTO samples and lithium metal foil were used for the working and counter electrodes, respectively. Electrochemical impedance spectroscopy (EIS) measurements were performed on the cells in the fully charged state at 2.2V using a Schlumberger model SI 1260 impedance/gain-phase analyzer connected to a Schlumberger model SI 1286 electrochemical interface. The amplitude of the a.c. signal was 5mV over the frequency range of 1 MHz and 10 mHz. Solid lines were determined from the CNLS fitting methods of the impedance spectra to the equivalent circuit.

The role of surface coating with carbon was further confirmed by impedance analysis. Fig. S11 shows the impedance spectra (Nyquist plots) of both LTO/C nanocomposite (LTO-OA2-750C) and uncoated, mesoporous LTO (LTO-scMeOH-600C). The impedance spectra of both the LTO materials were composed of two arcs and Warburg tail that appeared at the low frequency range. At high frequencies, the semicircles correspond to the resistance due to the passivation film on the lithium metal anode.[7, 29] The second semicircle in the middle frequency range is attributed to the charge transfer resistance.[3, 7]

Table S2. Impedance parameters derived using equivalent circuit model for the uncoated, mesoporous LTO (LTO-scMeOH-600C) and the core–shell LTO/C nanocomposite (LTO-OA2-750C)

Sample	R_s[a] (Ω)	R_f[b] (Ω)	R_{ct}[c] (Ω)
LTO-scMeOH-600C	3.2	5.2	142.9
LTO-OA2-750C	4.1	1.9	4.6

[a] R_s is solution resistance. [b] R_f is passivation film resistance.

[c] R_{ct} is charge-transfer resistance

References

1 A. Nugroho, S. J. Kim, K. Y. Chung, B.-W. Cho, Y.-W. Lee and J. Kim, *Electrochem. Commun.*, 2011, **13**, 650-653.

2 Y. G. Wang, H. M. Liu, K. X. Wang, H. Eiji, Y. R. Wang and H. S. Zhou, *J. Mater. Chem.*, 2009, **19**, 6789-6795.

3 H. Pan, L. Zhao, Y.-S. Hu, H. Li and L. Chen, *ChemSusChem*, 2012, **5**, 526-529.

4 L. Zhao, Y.-S. Hu, H. Li, Z. Wang and L. Chen, *Adv. Mater.*, 2011, **23**, 1385-1388.

5 L. Cheng, X. L. Li, H. J. Liu, H. M. Xiong, P. W. Zhang and Y. Y. Xia, *J. Electrochem. Soc.*, 2007, **154**, A692-A697.

6 L. Cheng, J. Yan, G.-N. Zhu, J.-Y. Luo, C.-X. Wang and Y.-Y. Xia, *J. Mater. Chem.*, 2010, **20**, 595-602.

7 E. Kang, Y. S. Jung, G.-H. Kim, J. Chun, U. Wiesner, A. C. Dillon, J. K. Kim and J. Lee, *Adv. Funct. Mater.*, 2011, **21**, 4349-4357.

8 T. Yuan, R. Cai and Z. P. Shao, *J. Phys. Chem. C*, 2011, **115**, 4943-4952.

9 Z. L. Jian, L. Zhao, R. Wang, Y. S. Hu, H. Li, W. Chen and L. Q. Chen, *RSC Adv.*, 2012, **2**, 1751-1754.

10 G.-N. Zhu, H.-J. Liu, J.-H. Zhuang, C.-X. Wang, Y.-G. Wang and Y.-Y. Xia, *Energy Environ. Sci.*, 2011, **4**, 4016-4022.

11 J. Wang, X. M. Liu, H. Yang and X. D. Shen, *J. Alloys Compd.*, 2011, **509**, 712-718.

12 T. Yuan, X. Yu, R. Cai, Y. K. Zhou and Z. P. Shao, *J. Power Sources*, 2010, **195**, 4997-5004.

13 X. Li, M. Z. Qu and Z. L. Yu, *Solid State Ionics*, 2010, **181**, 635-639.

14 H. Liu, Y. Feng, K. Wang and J. Y. Xie, *J. Phys. Chem. Solids*, 2008, **69**, 2037-2040.

15 G. J. Wang, J. Gao, L. J. Fu, N. H. Zhao, Y. P. Wu and T. Takamura, *J. Power Sources*, 2007, **174**, 1109-1112.

16 X. Li, M. Z. Qu, Y. J. Huai and Z. L. Yu, *Electrochim. Acta*, 2010, **55**, 2978-2982.

17 X. B. Hu, Z. J. Lin, K. R. Yang, Y. J. Huai and Z. H. Deng, *Electrochim. Acta*, 2011, **56**, 5046-5053.

18 M. R. Jo, K. M. Nam, Y. Lee, K. Song, J. T. Park and Y. M. Kang, *Chem. Commun.*, 2011, **47**, 11474-11476.

19 K. S. Park, A. Benayad, D. J. Kang and S. G. Doo, *J. Am. Chem. Soc.*, 2008, **130**, 14930-14931.

20 A. S. Prakash, P. Manikandan, K. Ramesha, M. Sathiya, J. M. Tarascon and A. K. Shukla, *Chem. Mater.*, 2010, **22**, 2857-2863.

21 S. L. Chou, J. Z. Wang, H. K. Liu and S. X. Dou, *J. Phys. Chem. C*, 2011, **115**, 16220-16227.

22 J. Kim and J. Cho, *Electrochem. Solid-State Lett.*, 2007, **10**, A81-A84.

23 J. Kim, Y.-S. Park, B. Veriansyah, J.-D. Kim and Y.-W. Lee, *Chem. Mater.*, 2008, **20**, 6301-6303.

24 B. Veriansyah, H. Park, J.-D. Kim, B. K. Min, Y. H. Shin, Y.-W. Lee and J. Kim, *J. Supercrit. Fluids*, 2009, **50**, 283-291.

25 N. R. Smyrl, E. L. Fuller and G. L. Powell, *Appl. Spectrosc.*, 1983, **37**, 38-44.

26 M. Q. Snyder, W. J. DeSisto and C. P. Tripp, *Appl. Surf. Sci.*, 2007, **253**, 9336-9341.

27 A. Nugroho, B. Veriansyah, S. K. Kim, B. G. Lee, J. Kim and Y.-W. Lee, *Chem. Eng. J.*, 2012, **193–194**, 146-153.

28 B. Veriansyah, J.-D. Kim, B. K. Min, Y. H. Shin, Y.-W. Lee and J. Kim, *J. Supercrit. Fluids*, 2010, **52**, 76-83.

29 N. Schweikert, H. Hahn and S. Indris, *Phys. Chem. Chem. Phys.*, 2011, **13**, 6234-6240.